Available online at www.sciencedirect.com

ScienceDirect

IFAC PapersOnLine 55-6 (2022) 329–334

Model-based thermal fault detection in Li-ion batteries using a set-based approach ⋆

Giacomo Saccani Diego Locatelli Angelo Tottoli Davide M. Raimondo

Department of Electrical, Computer and Biomedical Engineering, University of Pavia, Italy, (giacomo.saccani01@universitadipavia.it)

Abstract: Li-ion batteries suffer from reliability issues due to thermal instability. For this reason, it is important to design suitable Battery Management Systems (BMSs) able to enhance safety and guarantee high battery performance. In this paper we address the problem of detection of thermal faults within a Li-ion cell using a set-based fault detection scheme where unknown but bounded uncertainties are considered. In particular, an equivalent circuit model (ECM) is used for state estimation taking into account bounded parametric uncertainties and measurement noise. The proposed method relies on constrained zonotopes (CZ), a set representation useful for performing standard operations with a lower computational effort with respect to polytopes. Numerical simulations highlight the effectiveness of the proposed approach in detecting thermal faults at an early stage and show the benefits when compared to an interval based method relying on inclusion functions and constraint propagation.

Keywords: Fault detection, Li-ion batteries, set-membership estimation.

1. INTRODUCTION

One of the critical aspects to consider when operating Li-ion batteries is safety. Several faults can occur during battery operation which could result in significant performance degradation and potentially serious consequences, such as fires or explosions. Battery faults can be essentially of three types: cell faults, sensor faults and actuator faults. Cell faults are the most critical ones and include overcharging (OC), overdischarging (OD), overheating, external short circuit (ESC), internal short circuit (ISC) and thermal runaway (Hu et al., 2020). Sensor faults instead cause issues in the feedback loop of the BMS, that typically relies on sensor measurements (Xiong et al., 2019). Actuator faults include cooling system faults, bus faults and connector faults (Liu et al., 2014).

The device responsible for handling faults, as well as other operational aspects, is the BMS. The functioning principle is to take measures coming from the battery pack (voltage, current and temperature), analyze them and take decisions. The BMS can help in minimizing the effect of a fault and keep the battery operation inside a safe range using fault diagnostic and tolerant control methods.

Many fault diagnostic algorithms have been developed for Li-ion batteries, which can be divided in two different groups, based on the methodology on which they rely: data-driven and model-based. Data-driven methods are able to detect the faults by analyzing data without relying on a model. Wang et al. (2017) use Shannon entropy theory to capture thermal abnormalities and predict a fault. In Xiong et al. (2012), the authors propose a probabilistic rule-based method to find OD failures; the rules to detect faults assess unusual voltage drops and temperature rises. Big data statistical methods are employed in Zhao et al. (2017) to find abnormal changes of cell terminal voltages in a battery pack with a neural network algorithm. Note that the tuning of data-driven methods is usually time-consuming and costly, and therefore performed offline.

Model-based methods rely on mathematical models in order to capture the physical behaviour of the battery. These approaches are generally preferred to data-driven methods, because they provide a better insight and understanding of the nature of the fault. Moreover, they allow for an understandable design process and continuous validation at all stages of the method development. There exist many different models for Li-ion cells, varying in complexity and precision. Amongst the most notable there are ECMs and Electrochemical Models (EMs). While ECMs have fairly simple dynamics, they retain the ability of being simulated and used in real time applications. EMs, on the contrary, have an higher level of complexity and precision but their use online in BMS applications is still an open issue. Model-based fault detection strategies compare measures coming from the battery pack with the ones generated by the mathematical model. The potential difference is then analyzed to determine whether a fault has occurred. In the literature, several works have tackled this problem using different approaches. In Dey et al. (2015), the authors analyze thermal faults in a single cell using the residual method with a nonlinear Luenberger-type observer to estimate core temperature. The nominal model is generated by an ECM. For the same conditions, a sliding mode observer is used in Marcicki et al. (2010) to identify sensor faults. In Singh et al. (2013) and Couto and Kinnaert (2018), respectively OC and OD, internal

⋆ This work has been partially supported by the Italian Ministry for Research in the framework of the 2017 PRIN, Grant no. 2017YKXYXJ.

10.1016/j.ifacol.2022.07.150

and sensor faults are identified using a linear Kalman filter (KF) as an observer; the first work uses an ECM to generate the nominal measure signals, while the second one uses an EM. In Dey et al. (2017) thermal faults are identified using a nonlinear Lyapunov observer, that allows to account for Gaussian uncertainties on the model. In all of these works, the faults are considered to be abrupt, meaning that they happen instantly and are not incremental.

One of the issues related to model-based fault-detection is the fact that the mathematical models are inaccurate. Moreover, measurement uncertainties provide an additional layer of unpredictability. Most of the approaches proposed in the literature either do not take into account any uncertainty or rely on the hypothesis that the distribution is known a priori. However, this is not realistic in general. On the other side, set-based approaches do not require knowledge of the distributions but rely on the assumption of unknown but bounded uncertainties only. In many cases, e.g. physical bounds, such assumption is reasonable and appears appropriate in the context of battery state estimation. Different set representations are available in literature: polytopes (Shamma and Tu, 1997), intervals (Jaulin et al., 2001), zonotopes (Alamo et al., 2008) and CZs (Scott et al., 2016). These representations differ in precision and computational effort. In the context of Li-ion batteries, interval based approaches have been used for state of charge (SOC) estimation of a single cell in Rausch et al. (2014) and in Locatelli et al. (2021) for all the states of the cell. The work of Zhang et al. (2021) uses an interval observer to estimate states of a battery, including thermal dynamics. An interval PDE observer is implemented in Perez and Moura (2015), for state estimation of an EM. To the extent of our knowledge, set-based estimation has never been used for fault detection in batteries.

The set-based approach we propose is based on CZs, that are used to detect thermal faults. CZs have the advantage of combining the efficiency and scalability of zonotopes with the flexibility of convex polytopes. Therefore, they represent an efficient methodology which is able to compute significantly tighter enclosures than e.g. intervals, at modest additional cost (Scott et al., 2016). In our work, only thermal faults were considered, however this methodology can be generalized to any other type of fault. To further validate the results, a comparison is proposed between CZs and interval sets; these latter are computed with a forward-backward algorithm according to Jaulin et al. (2001). Note that having enclosures as tight as possible is essential for having an early fault detection.

Summarizing, the novelty of this work consists of i) Application of novel set-based methods to battery state estimation, ii) Set-based fault detection in batteries, iii) Performance comparison in fault detection between interval sets and CZs.

2. LITHIUM-ION CELL MODEL

In this section we present the mathematical model used to describe the Li-ion cell behaviour. We consider a coupled electro-thermal model which consists of a second-order ECM augmented with a two-state thermal model describing the core and surface temperature dynamics.

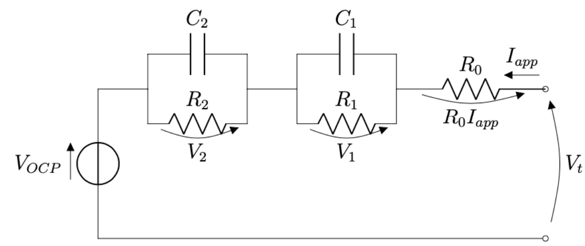

Fig. 1. Dual Polarization Equivalent Circuit Model

The ECM considered in this work is the Dual Polarization (DP) model schematized in Figure 1. Three elements can be distinguished: (i) the open circuit potential $V_{\mathrm{OCP}}(t)$; (ii) two parallel resistor-capacitor (RC) blocks; (iii) the internal ohmic resistance R_0. The current flowing in the cell $I_{app}(t)$ is assumed to be the known input of the system and is denoted with $u(t)$, positive if the cell is charging. The equations that describe the system are:

$$\dot{V}_1(t) = -\frac{V_1(t)}{R_1 C_1} + \frac{u(t)}{C_1}, \tag{1}$$

$$\dot{V}_2(t) = -\frac{V_2(t)}{R_2 C_2} + \frac{u(t)}{C_2}, \tag{2}$$

$$\dot{\mathrm{SOC}}(t) = \frac{u(t)}{C_{batt}}, \tag{3}$$

$$V_t(t) = V_{\mathrm{OCP}}(\mathrm{SOC}(t)) + V_1(t) + V_2(t) + R_0 u(t). \tag{4}$$

State of Charge (SOC) is defined as the level of charge in a cell, relative to its capacity C_{batt}. Note that, for the remainder of the paper, we will use the notation $\mathrm{SOC}(t) = z$. The open-circuit potential V_{OCP} is a non-linear polynomial function of z:

$$V_{\mathrm{OCP}}(z) = a + b \cdot z + c \cdot z^2 + d \cdot z^3 + e \cdot z^4 + f \cdot z^5 + \\ + g \cdot z^6 + h \cdot z^7 + i \cdot z^8 + j \cdot z^9, \tag{5}$$

The thermal model used is this paper is the one proposed in Lin et al. (2014). Model equations can be written as follows

$$\dot{T}_c(t) = \frac{T_s(t) - T_c(t)}{R_c C_c} + \frac{|u(t)||(V_t(t) - V_{\mathrm{OCP}}(z))|}{C_c}, \tag{6}$$

$$\dot{T}_s(t) = \frac{T_f(t) - T_s(t)}{R_u C_s} - \frac{T_s(t) - T_c(t)}{R_c C_s}, \tag{7}$$

where R_c is the heat conduction resistance that represents the heat exchange between the core and the surface, R_u is convection resistance used to model convective cooling between T_s and T_f (ambient temperature); C_c and C_s are respectively the core and surface heat capacity. This thermal model is a simplification, as the temperature is assumed uniform in the core and on the surface. Moreover, we assume that the surface of the cell is in contact with the external air, at a constant temperature. The values for the parameters will be defined in Section 5.

2.1 Fault model

As mentioned before, different types of faults are possible. In this work, we focus only on thermal ones and rely on the work of Dey et al. (2015). In particular, three thermal faults were there considered:

- *Fault 1*: R_u significantly deviates from its nominal value, representing a convective cooling fault;
- *Fault 2*: R_c significantly deviates from its nominal value, representing an internal thermal resistance fault;
- *Fault 3*: an additional heat generation term contributes to the rise of the core temperature T_c, causing thermal runaway.

The modified thermal model including the presence of these faults is reported below:

$$C_c\dot{T}_c(t) = \frac{T_s(t) - T_c(t)}{(R_c + \Delta R_c)} + |u(t)||(V_t(t) - V_{\mathrm{OCP}}(z))| + \Delta r,$$
$$C_s\dot{T}_s(t) = \frac{T_f(t) - T_s(t)}{(R_u + \Delta R_u)} + \frac{T_s(t) - T_c(t)}{R_c + \Delta R_c}, \tag{8}$$

where ΔR_c and ΔR_u represent the first two faults, while Δr represents thermal runaway. It is assumed that multiple faults cannot occur at the same time and that faults happen suddenly, meaning that at a certain time instant, the faulty value will be instantly shifted by a certain amount. Note that faults are mutually causal, and can create a cascading effect. However, in this work we will also assume that fault detection is fast enough to avoid it.

3. PRELIMINARIES TO SET-BASED ESTIMATION

In this section we recall some notions necessary to understand the proposed set-based approach for the detection of thermal faults in a Li-ion cell. Both interval and CZs are here presented since Section 5 will compare the results obtained using these two classes of sets.

3.1 Interval analysis

Consider $\underline{x}$, $\overline{x} \in \mathbb{R}$, such that $\underline{x} \leq \overline{x}$. An interval $[x] \subset \mathbb{R}$ is a nonempty set of real numbers denoted as $[x] \triangleq \{x \in \mathbb{R} : \underline{x} \leq x \leq \overline{x}\}$. Moreover, the midpoint and the radius of an interval $[x]$ are defined by $\mathrm{mid}([x]) \triangleq 0.5(\overline{x} + \underline{x})$ and $\mathrm{rad}([x]) \triangleq 0.5(\overline{x} - \underline{x})$, respectively. The set of all intervals over $\mathbb{R}$ is indicated by $\mathbb{IR}$. The set of all interval vectors in $\mathbb{R}^n$ is defined as $\mathbb{IR}^n$. A box $[X] \in \mathbb{IR}^n$ is denoted with $[X] = ([\underline{x}_1, \overline{x}_1], \ldots, [\underline{x}_n, \overline{x}_n])$. The radius and midpoint of $[X]$ are defined by $\mathrm{rad}([X]) \triangleq (\mathrm{rad}([\underline{x}_1, \overline{x}_1]), \ldots, \mathrm{rad}([\underline{x}_n, \overline{x}_n])$ and $\mathrm{mid}([X]) \triangleq (\mathrm{mid}([\underline{x}_1, \overline{x}_1]), \ldots, \mathrm{mid}([\underline{x}_n, \overline{x}_n])$, respectively. A real arithmetic operation $\odot$ is extended to intervals $[x_1], [x_2] \in \mathbb{IR}$ by $[x_1] \odot [x_2] \triangleq \{x_1 \odot x_2 : x_1 \in [x_1], x_2 \in [x_2]\}$. The intersection of two intervals is defined as $[x_1] \cap [x_2] \triangleq [\max\{\underline{x}_1, \underline{x}_2\}, \min\{\overline{x}_1, \overline{x}_2\}]$. Inclusion functions and basic operations are detailed in Moore et al. (2009).

3.2 Constrained zonotopes and set operations

Definition 1. *Let $P, Z, Z_c \subset \mathbb{R}^n$. P is a* convex polytope *if it is bounded and* (9) *holds; Z is a zonotope if* (10) *holds and Z_c is a CZ if* (11) *holds.*

$$\exists(\mathbf{H}, \mathbf{k}) \in \mathbb{R}^{n_h \times n} : P = \{\boldsymbol{z} \in \mathbb{R}^n : \mathbf{H}\boldsymbol{z} \leq \mathbf{k}\}, \tag{9}$$
$$\exists(\mathbf{G}, \boldsymbol{c}) \in \mathbb{R}^{n \times n_g} \times \mathbb{R}^n : Z = \{\boldsymbol{c} + \mathbf{G}\boldsymbol{\xi} : \|\boldsymbol{\xi}\|_\infty \leq 1\}, \tag{10}$$
$$\begin{aligned}&\exists(\mathbf{G}, \boldsymbol{c}, \mathbf{A}, \boldsymbol{b}) \in \mathbb{R}^{n \times n_g} \times \mathbb{R}^n \times \mathbb{R}^{n_c \times n_g}, \times \mathbb{R}^{n_c} : \\ &\quad Z_c = \{\boldsymbol{c} + \mathbf{G}\boldsymbol{\xi} : \|\boldsymbol{\xi}\|_\infty \leq 1, \mathbf{A}\boldsymbol{\xi} = \boldsymbol{b}\}.\end{aligned} \tag{11}$$

Note that (9) expresses the convex polytope P through the halfspace-representation (H-rep) but this can also be obtained as the convex hull of its vertices (V-rep). Zonotopes are centrally symmetric convex polytopes expressed in (10) with the so called *generator representation* (G-rep), where $\mathbf{G}$ is the *generator matrix*, $\boldsymbol{\xi}$ the *generators vector* and $\boldsymbol{c}$ the zonotope *center*. CZs are an extension of zonotopes which consider linear equality constraints on $\boldsymbol{\xi}$. This feature allows CZs to describe any arbitrary convex polytope when no restriction on the number of generators/constraints is provided (in terms of generators and constraints) (Scott et al., 2016). Equation (11) defines a CZ using the so called *constrained generator representation* (CG-rep) where $\mathbf{A}\boldsymbol{\xi} = \boldsymbol{b}$ are the *constraints*. Note that it is possible to interpret a zonotope and a CZ as respectively the image, under an affine mapping, of a unit hypercube B_∞ and a constrained unit hypercube $B_\infty(\mathbf{A}, \boldsymbol{b}) \equiv \{\boldsymbol{\xi} \in B_\infty : \mathbf{A}\boldsymbol{\xi} = \boldsymbol{b}\}$ in $\mathbb{R}^{n_g}$. From here on, the shorthand $Z_c = \{\mathbf{G}_z, \boldsymbol{c}_z, \mathbf{A}_z, \boldsymbol{b}_z\}$, and $Z = \{\mathbf{G}, \boldsymbol{c}\}$ will be used to indicate CZs and zonotopes respectively. Let $Z, W \subset \mathbb{R}^n$, $Y \subset \mathbb{R}^m$, and $\mathbf{R} \in \mathbb{R}^{m \times n}$, then

$$\mathbf{R}Z \triangleq \{\mathbf{R}\boldsymbol{z} : \boldsymbol{z} \in Z\}, \tag{12}$$
$$Z \oplus W \triangleq \{\boldsymbol{z} + \boldsymbol{w} : \boldsymbol{z} \in Z, \boldsymbol{w} \in W\}, \tag{13}$$
$$Z \cap_{\mathbf{R}} Y \triangleq \{\boldsymbol{z} \in Z : \mathbf{R}\boldsymbol{z} \in Y\}, \tag{14}$$

where (12) denotes the linear image of Z, (13) the Minkowski sum of sets and (14) the generalized intersection according to Scott et al. (2016). Using intervals the Minkowski sum can be computed exactly, but (12) and (14) are conservative due to the wrapping effect. In contrast, convex polytopes are closed under (12)-(14), but these operations can be very costly and numerically unstable in high dimensions. On the other side, these operations can be easily computed in CG-rep as follows

$$\mathbf{R}Z = \{\mathbf{R}\mathbf{G}_z, \mathbf{R}\boldsymbol{c}_z, \mathbf{A}_z, \boldsymbol{b}_z\}, \tag{15}$$
$$Z \oplus W = \left\{[\mathbf{G}_z \ \mathbf{G}_w], \boldsymbol{c}_z + \boldsymbol{c}_w, \begin{bmatrix}\mathbf{A}_z & \mathbf{0} \\ \mathbf{0} & \mathbf{A}_w\end{bmatrix}, \begin{bmatrix}\boldsymbol{b}_z \\ \boldsymbol{b}_w\end{bmatrix}\right\}, \tag{16}$$
$$Z \cap_{\mathbf{R}} Y = \left\{[\mathbf{G}_z \ \mathbf{0}], \boldsymbol{c}_z, \begin{bmatrix}\mathbf{A}_z & \mathbf{0} \\ \mathbf{0} & \mathbf{A}_y \\ \mathbf{R}\mathbf{G}_z & -\mathbf{G}_y\end{bmatrix}, \begin{bmatrix}\boldsymbol{b}_z \\ \boldsymbol{b}_y \\ \boldsymbol{c}_y - \mathbf{R}\boldsymbol{c}_z\end{bmatrix}\right\}. \tag{17}$$

See Scott et al. (2016) for further details on CZs.

4. SET-BASED ESTIMATION AND FAULT DETECTION

Consider a class of nonlinear discrete-time systems described by the following equations

$$\begin{aligned}\boldsymbol{x}_k &= \boldsymbol{f}(\boldsymbol{x}_{k-1}, \boldsymbol{u}_{k-1}, \boldsymbol{w}_{k-1}) \quad &\text{for} \quad k \geq 1, \\ \boldsymbol{y}_k &= \boldsymbol{g}(\boldsymbol{x}_k, \boldsymbol{u}_k, \boldsymbol{v}_k) \quad &\text{for} \quad k \geq 0,\end{aligned} \tag{18}$$

where $\boldsymbol{x}_k \in \mathbb{R}^{n_x}$ is the system state vector, $\boldsymbol{u}_k \in \mathbb{R}^{n_u}$ are the known inputs, $\boldsymbol{y}_k \in \mathbb{R}^{n_y}$ indicates the measured outputs, while $\boldsymbol{w}_k \in \mathbb{R}^{n_w}$ and $\boldsymbol{v}_k \in \mathbb{R}^{n_v}$ denote process and output uncertainties respectively. We assume that the initial condition $\boldsymbol{x}_0 \in X_0$ and the disturbances are bounded by $\boldsymbol{w}_k \in W$ and $\boldsymbol{v}_k \in V$, where X_0, W and V are known compact sets. The objective of set-based state estimation is to compute, at each $k \geq 0$, tight enclosures $\hat{X}_k$ of the set of states consistent with the model dynamics, the bounded uncertainties X_0, W, V and the collected measurements $\boldsymbol{y}_k$. This is done through a prediction-update algorithm, that computes the compact sets $\bar{X}_k$ and $\hat{X}_k$ as follows

$$\bar{X}_k \supseteq \{\mathbf{f}(\mathbf{x}, \mathbf{u}_{k-1}, \mathbf{w}_{k-1}) : \mathbf{x} \in \hat{X}_{k-1}, \boldsymbol{w}_{k-1} \in W\}, \quad (19)$$

$$\hat{X}_k \supseteq \{\boldsymbol{x} \in \bar{X}_k : \mathbf{g}(\mathbf{x}, \mathbf{u}_k, \mathbf{v}_k) = \mathbf{y}_k, \mathbf{v}_k \in V\}, \quad (20)$$

in which (19) and (20) are referred to as *prediction step* and *update step* respectively. Note that, in general, the set operations defined in (19)-(20) cannot be evaluated exactly. This is why tight guaranteed enclosures (meaning, in this context, tight outer approximations) are computed instead. Within this respect, CZs have shown significant advantages over other set representations (Scott et al., 2016). The details on how to perform the prediction-update algorithm for nonlinear discrete-time systems using CZs can be found in Rego et al. (2021). This procedure has been used in order to obtain a set-based state estimation scheme for the cell model reported in Section 2.

Set-based fault detection consists in evaluating the consistency of the obtained measurements $\mathbf{y}_k$ with the predicted output set generated by the nominal (healthy) dynamics, i.e. it consists in performing, at each k, the inclusion check

$$\mathbf{y}_k \in \mathbf{g}(\bar{X}_k, \mathbf{u}_k, V). \quad (21)$$

A fault is detected when the measurement does not lie in the output set, i.e. $\mathbf{y}_k \notin \mathbf{g}(\bar{X}_k, \mathbf{u}_k, V)$ or, equivalently, when the update step (20) results in $\hat{X}_k$ being empty. The accuracy of the set-based estimation is fundamental in order to achieve an early fault detection, thus limiting the consequences related to the fault. The motivation for using CZs is therefore apparent. Since CZ can provide tighter enclosures compared to zonotopes and intervals, at the price of a mild increase in complexity, they can lead to an earlier detection. In the following we demonstrate the advantages of a set-based approach based on CZs over an interval method, based on a forward-backward algorithm (see Jaulin et al. (2001)), in the detection of thermal faults in a Li-ion cell.

5. NUMERICAL RESULTS

In this section, the proposed method is applied to the model described in Section 2 and numerical results are presented. For what concerns the parameters used, some considerations are needed. When dealing with mathematical models, the parameter identification may lead to an imprecision in the estimated parameter values. This fact can be taken into account in the model by considering parametric uncertainties. The base value for electrical and thermal parameters as well as the V_{OCP} coefficients were taken from Lin et al. (2014) [1] and they are reported in Tables 1 and 2 respectively. The uncertainty was set for each parameter in Table 1 to $\pm 2.5\%$. The external air temperature is set at $T_f = 298.15$K. As it happens in a real case scenario, the measurable quantities are terminal voltage V_t and surface temperature T_s. The measurement noise has been set respectively to $\pm 1\ mV$ and $\pm 0.1\ K$. We assume that the initial state condition is uncertain and lies in the zonotope

$$\bar{X}_0 = \{\mathbf{G}_{x_0}, \mathbf{c}_{x_0}\}, \quad (22)$$

[1] The coefficients in Eq. (5) have been obtained by interpolation

Param.	Value	Unit	Param.	Value	Unit
C_1	2100	Ah	C_2	70000	Ah
C_{bat}	2.3	Ah	R_0	0.01	Ω
R_1	0.02	Ω	R_2	0.02	Ω
R_u	3.08	KW^{-1}	R_c	1.94	KW^{-1}
C_c	62.7	JK^{-1}	C_s	4.5	JK^{-1}

Table 1. Electro-thermal model parameters

Coeff.	a	b	c	d	e
Value	2.611	17.04	-204.4	1369	-5423
Coeff.	f	g	h	i	j
Value	13210	-19970	18260	-9247	1990

Table 2. Coefficient values for $V_{\text{OCP}}(z)$

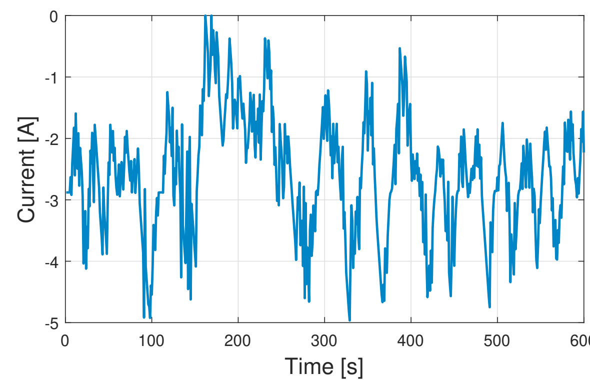

Fig. 2. Input current profile $u(t)$ applied to the cell.

with $\mathbf{G}_{x_0} = \text{diag}([0.001\ 0.001\ 0.05\ 1\ 1])$ and $\mathbf{c}_{x_0} = [0.005\ 0.005\ 0.25\ 298.15\ 298.15]^\intercal$. In particular, for the zonotope center the SOC has been set equal to 0.25 and both core and surface temperature to ambient temperature.

All the simulations described in the following rely on the input current profile reported in Figure 2. This profile can represent an electric vehicle driving cycle. The cell parameters used for simulating the healthy cell were extracted randomly within the parameter bounds mentioned above. Similarly, the initial condition used in all the simulations was extracted randomly within $\bar{X}_0$. Measurements were obtained by simulating the cell nominal and faulty models (the ones reported in Section 2.1) in a time interval of $[0, 600]$ seconds. The fault was injected at $k = 200\ s$.

In Figure 3 we show the CZ set-based estimation approach applied in open-loop (i.e. by performing the prediction step (19) only) and in closed-loop (i.e. by performing both prediction and update steps (20)) to the Li-ion cell model. The figure provides the projection of the sets in the state-space of V_1, V_2 and SOC at $k = \{2, 12, 22, 42, 95\}$; in blue are depicted the open-loop sets, while in yellow the closed-loop enclosures. As expected, these latter include a much smaller volume, as the system output measurement allows to restrict the feasible state values. Moreover, differently from intervals, CZs are able to capture the dependency between state variables, thus reducing conservatism.

Finally, we can analyze the effectiveness of the proposed method in detecting faults and compare the performance of intervals and CZs. In Figure 5, the output space (that

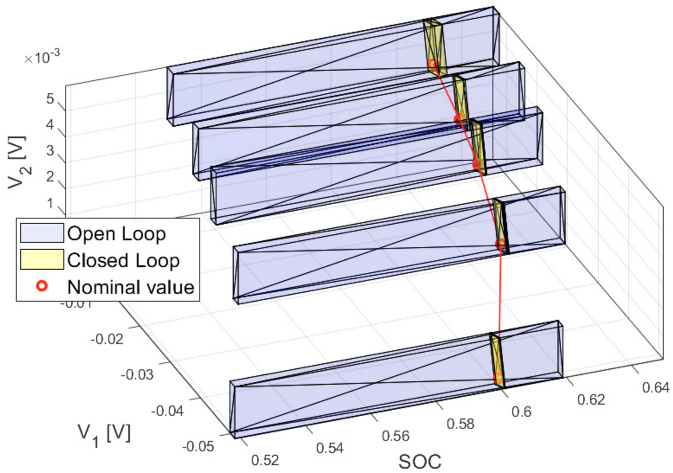

Fig. 3. Comparison between open-loop and closed-loop state trajectories using CZ.

Magnitude	Detection	Magnitude	Detection
$\Delta R_u = -30\%$	$4\ s$	$\Delta R_u = -45\%$	$3\ s$
$\Delta R_c = -30\%$	$6\ s$	$\Delta R_c = -45\%$	$5\ s$
$\Delta r = 0.01\ K$	$16\ s$	$\Delta r = 0.1\ K$	$6\ s$

Table 3. Time needed for the developed method to detect the fault.

includes V_t and T_s) is represented for the case of Fault 1 (similar results have been obtained in the other cases); the red line represents the measure coming from the cell, while in green and yellow respectively we have interval and CZ sets. These are obtained by a mean value extension (see Rego et al. (2021)) of the output function, using the predicted states $\bar{X}_k$, i.e. the set in equation (21). Interval sets instead are obtained solving the constraint satisfaction problem and using the forward-backward algorithm in Jaulin et al. (2001). When the measure coming from the system does not lie inside these sets, the fault has been detected. The first observation is that intervals are very conservative in the prediction step: their size (and therefore, the feasible output values) increases during the simulation, making fault detection practically impossible.

In order to assess the effectiveness of the CZ-based strategy in detecting the considered faults, an analysis was performed for different fault magnitudes. The instant in which the fault is detected is provided in Table 3 (the resistive fault is in percentage of the base value). As expected, we can see that the bigger the fault, the fastest the detection time is. Unfortunately, in all the considered cases, the interval-based method was not able to detect the faults.

In Figure 4 the radius[2] of the output sets defined in (21), obtained using intervals and CZs, are depicted for every time instant within the time window $[0, 200]s$. As it can be noticed, the intervals explode over time. When analyzing the reasons of such explosion, we notice that a significant growth of the bounds along the component of T_c occurs in the prediction phase. This is due to the parameter uncertainty present in the system. While the update phase should reduce such uncertainty, intervals are refined only on the state components that explicitly

[2] This is computed as half the length of the longest edge of the interval hull, as in Scott et al. (2016).

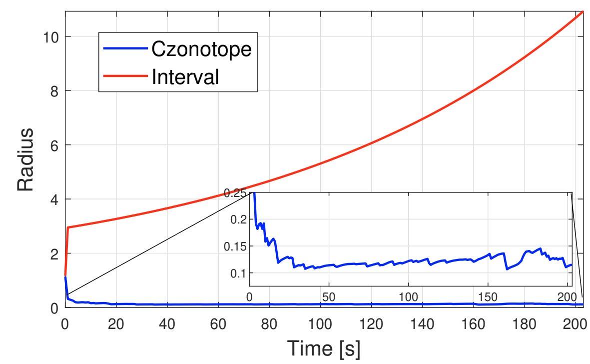

Fig. 4. Comparison between radii of interval and CZ on the output (Fault 1).

appear in the output equation (see Locatelli et al. (2021)). Because this is not the case for T_c, the result is that it never gets refined and the closed-loop and open-loop estimation are the same for that component. A bad estimation of T_c heavily affects also the estimation of the other sets. This fact makes it impossible to detect the fault with the interval method, because if the set is big, the measure will always be consistent with the prediction (i.e. lies in the set).

Finally, note that the prediction-update scheme requires on average 0.6061s for CZs and 0.0409s for intervals using the method in Jaulin et al. (2001). As expected intervals are computationally cheaper. However, within this context, they do not represent a viable solution since, due to their conservativeness, are unable to detect the considered faults.

6. CONCLUSIONS

In this work we demonstrated the advantages of constrained zonotopes over intervals in the detection of thermal faults in Li-ion cells. As highlighted by the results, constrained zonotopes are able to provide a set-based estimation which results in tight enclosures where, differently from intervals, it is possible to capture the coupling between the different state components. This feature, even in the presence of parameter uncertainties, allows to detect faults in a very effective way.

ACKNOWLEDGEMENTS

We thank Dr. B. S. Rego and Prof. G. V. Raffo from Universidade Federal de Minas Gerais for providing support with methodology and useful suggestions. The assistance provided by Eng. A. Genovese from ENEA was also appreciated.

REFERENCES

Alamo, T., Bravo, J.M., Redondo, M.J., and Camacho, E.F. (2008). A set-membership state estimation algorithm based on dc programming. *Automatica*, 44(1), 216–224.

Couto, L.D. and Kinnaert, M. (2018). Internal and sensor fault detection and isolation for li-ion batteries. *IFAC-PapersOnLine*, 51(24), 1431–1438.

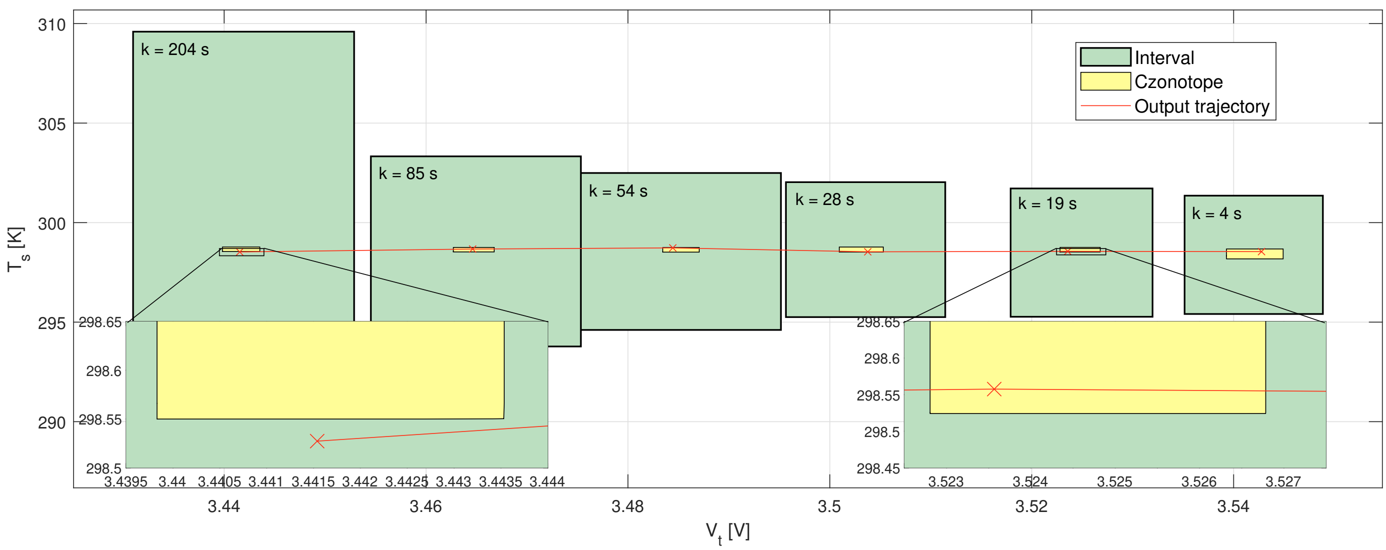

Fig. 5. Comparison between interval and CZ on output trajectories (Fault 1).

Dey, S., Biron, Z.A., Tatipamula, S., Das, N., Mohon, S., Ayalew, B., and Pisu, P. (2015). On-board thermal fault diagnosis of lithium-ion batteries for hybrid electric vehicle application. *IFAC-PapersOnLine*, 48(15), 389–394.

Dey, S., Perez, H.E., and Moura, S.J. (2017). Model-based battery thermal fault diagnostics: Algorithms, analysis, and experiments. *IEEE Transactions on Control Systems Technology*, 27(2), 576–587.

Hu, X., Zhang, K., Liu, K., Lin, X., Dey, S., and Onori, S. (2020). Advanced fault diagnosis for lithium-ion battery systems: a review of fault mechanisms, fault features, and diagnosis procedures. *IEEE Industrial Electronics Magazine*, 14(3), 65–91.

Jaulin, L., Braems, I., Kieffer, M., and Walter, E. (2001). Nonlinear state estimation using forward-backward propagation of intervals in an algorithm. In *Scientific computing, validated numerics, interval methods*, 191–201. Springer.

Lin, X., Perez, H.E., Mohan, S., Siegel, J.B., Stefanopoulou, A.G., Ding, Y., and Castanier, M.P. (2014). A lumped-parameter electro-thermal model for cylindrical batteries. *Journal of Power Sources*, 257, 1–11.

Liu, Z., Ahmed, Q., Rizzoni, G., and He, H. (2014). Fault detection and isolation for lithium-ion battery system using structural analysis and sequential residual generation. In *Dynamic Systems and Control Conference*, volume 46193. American Society of Mechanical Engineers.

Locatelli, D., Rego, B., Raffo, G., and Raimondo, D. (2021). Interval state estimation based on constraint propagation for a lithium-ion cell using an equivalent circuit model. *IFAC-PapersOnLine*, 54(3), 602–608.

Marcicki, J., Onori, S., and Rizzoni, G. (2010). Nonlinear fault detection and isolation for a lithium-ion battery management system. In *Dynamic Systems and Control Conference*, volume 44175, 607–614.

Moore, R.E., Kearfott, R.B., and Cloud, M.J. (2009). *Introduction to Interval Analysis*. SIAM, Philadelphia, PA, USA.

Perez, H.E. and Moura, S.J. (2015). Sensitivity-based interval pde observer for battery soc estimation. In *2015 American Control Conference (ACC)*, 323–328. IEEE.

Rausch, M., Klein, R., Streif, S., Pankiewitz, C., and Findeisen, R. (2014). Set-based state of charge estimation for lithium-ion batteries. In *2014 American Control Conference*, 1566–1571. IEEE.

Rego, B.S., Scott, J.K., Raimondo, D.M., and Raffo, G.V. (2021). Set-valued state estimation of nonlinear discrete-time systems with nonlinear invariants based on constrained zonotopes. *Automatica*, 129, 109638.

Scott, J.K., Raimondo, D.M., Marseglia, G.R., and Braatz, R.D. (2016). Constrained zonotopes: A new tool for set-based estimation and fault detection. *Automatica*, 69, 126–136.

Shamma, J.S. and Tu, K.Y. (1997). Approximate set-valued observers for nonlinear systems. *IEEE transactions on automatic control*, 42(5), 648–658.

Singh, A., Izadian, A., and Anwar, S. (2013). Fault diagnosis of li-ion batteries using multiple-model adaptive estimation. In *IECON 2013-39th Annual Conference of the IEEE Industrial Electronics Society*, 3524–3529. IEEE.

Wang, Z., Hong, J., Liu, P., and Zhang, L. (2017). Voltage fault diagnosis and prognosis of battery systems based on entropy and z-score for electric vehicles. *Applied energy*, 196, 289–302.

Xiong, J., Banvait, H., Li, L., Chen, Y., Xie, J., Liu, Y., Wu, M., and Chen, J. (2012). Failure detection for over-discharged li-ion batteries. In *2012 IEEE International Electric Vehicle Conference*, 1–5. IEEE.

Xiong, R., Yu, Q., Shen, W., Lin, C., and Sun, F. (2019). A sensor fault diagnosis method for a lithium-ion battery pack in electric vehicles. *IEEE Transactions on Power Electronics*, 34(10), 9709–9718.

Zhang, D., Couto, L.D., Gill, P.S., Benjamin, S., Zeng, W., and Moura, S.J. (2021). Thermal-enhanced adaptive interval estimation in battery packs with heterogeneous cells. *IEEE Transactions on Control Systems Technology*, 1–14.

Zhao, Y., Liu, P., Wang, Z., Zhang, L., and Hong, J. (2017). Fault and defect diagnosis of battery for electric vehicles based on big data analysis methods. *Applied Energy*, 207, 354–362.